JOURNAL OF Materials CHEMISTRY

Dimethylamino- and trimethylammonium-tipped oxyethylene–oxybutylene diblock copolymers and their use as structure-directing agents in the preparation of mesoporous silica

Carin E. Tattershall, Sumera J. Aslam and Peter M. Budd*

Department of Chemistry, The University of Manchester, Manchester, UK M13 9PL. E-mail: Peter.Budd@man.ac.uk

Received 12th March 2002, Accepted 25th April 2002
First published as an Advance Article on the web 29th May 2002

Oxyethylene–oxybutylene diblock copolymers with a dimethylamino tip to the hydrophilic block were prepared by anionic polymerization, using aminoalcohol initiators in a dry aprotic medium. Conversion of a high percentage of the alcohol to alkoxide minimized the formation of unwanted by-products, but slightly broadened the molar mass distribution of the copolymers. Trimethylammonium-tipped copolymers were prepared by quaternization with methyl iodide. The copolymers were utilised as structure-directing agents in the preparation of silica under acidic conditions, where all the copolymers carry a positive charge, and subsequent removal of the copolymers by calcination gave mesoporous materials. The silica mesostructure depended on the relative sizes of the polymer blocks, changing from body-centred cubic to three-dimensional hexagonal to two-dimensional hexagonal on decreasing the proportion of hydrophilic units. The overall silica mesostructure dimensions, as determined from X-ray analysis, increased with an increase in micelle size, and the mesopore dimensions, as determined from nitrogen adsorption analysis, increased with an increase in the size of the core hydrophobic block. A simple model is suggested in which the hydrophilic chains are embedded in the silica walls in the uncalcined silica, generating micropores on calcination, whilst the hydrophobic chains form a separate microphase, giving rise to mesopores on calcination. The effect of charged tips, as compared with equivalent nonionic diblock copolymers, is to expand the dimensions of the mesostructures obtained and to generate higher surface areas in the calcined silica products.

Introduction

Block copolymers are of considerable interest for their ability to self-organize into well-defined superstructures.[1] In dilute solution in a selective solvent, amphiphilic block copolymers form micelles. In concentrated solution, a variety of superstructures may be encountered, including body-centred cubic (bcc) or face-centred cubic (fcc) arrays of spherical micelles, hexagonal arrays of elongated micelles, lamellar structures and bicontinuous cubic (*e.g.*, gyroid) structures. The association behaviour of diblock, triblock and cyclic copolymers incorporating hydrophilic blocks of oxyethylene (E), –[OCH_2CH_2]– units and hydrophobic blocks of oxybutylene (B), –[$OCH_2CH(C_2H_5)$]– or oxypropylene (P), –[$OCH_2CH(CH_3)$]–, units has been extensively studied.[2] A B unit may be regarded as being about six times more hydrophobic than a P unit.[3]

The ability of amphiphiles to form organized structures may be utilized in the preparation of mesostructured inorganic materials. Subsequent removal of the amphiphile by calcination or solvent-extraction yields ordered, mesoporous materials that show considerable potential for application in separations and catalysis.[4,5] Interest in the use of amphiphiles as structure-directing agents was sparked by reports of the preparation at Mobil of hexagonal (MCM-41), lamellar (MCM-50) and bicontinuous cubic (MCM-48) silicas, utilizing cationic surfactants.[6,7] The concept has been extended to the formation of a variety of metal oxide structures and to the use of different types of amphiphile, including $E_mP_nE_m$ triblock copolymers.[8–10] We have undertaken a systematic study of the use of E–B diblock and triblock copolymers as structure-directing agents in the preparation of mesostructured precipitates, and have demonstrated the principle of fine-tuning the structure, mesostructure dimensions, surface properties and morphology of the mesoporous product through control of the composition and architecture of the polymer.[4,11] The mechanism of formation of mesostructured precipitates is a subject of debate, our current view being that it is best understood as a process of liquid–liquid separation followed by microphase separation within the concentrated phase.[5]

The superstructure formed by block copolymer micelles in concentrated solution depends on geometrical factors and on the interaction potential. In general, it has been found for E_mB_n copolymers that when corona blocks are large relative to the core ($m/n \geqslant 10$) the micelles act as 'soft spheres' and a bcc structure is obtained, whilst copolymers with shorter corona blocks give micelles that behave as 'hard spheres' (short-range repulsive interactions dominate) and form fcc structures at low concentration.[12] Very short corona blocks promote a transition from spherical to elongated micelles, and a hexagonal phase is then the first mesophase encountered on increasing the amphiphile concentration.

The effect of modifying the hydrophilic E block with a cationic tip has not previously been studied. Incorporation of a cationic group will introduce long-range interactions that may be expected to influence the phase behaviour of the copolymer and modify the structure and surface properties of mesoporous materials generated with it. In the present work, a range of dimethylamino- and trimethylammonium-tipped E–B diblock copolymers were prepared and utilised as structure-directing agents. Silica was synthesised under acid conditions, where these copolymers will all be in cationic form, and the results compared with previous studies of nonionic copolymers.

Anionic polymerization of alkylene oxides is commonly initiated by an alcohol (ROH) that is partly in the form of its alkali-metal salt (*e.g.*, RO^-K^+). In the propagation reaction, the active centre is an ion pair. There is a very rapid transfer reaction between alkoxide ion and alcohol. Under the usual conditions of polymerization, at any given instant only a small

 DOI: 10.1039/b202455a

proportion of molecules are in the active alkoxide form, but rapid equilibration means that every molecule present has an equal chance of being in the alkoxide state. Consequently, a narrow distribution of chain lengths can be achieved. The polymerization of propylene oxide (PO) is complicated by a hydrogen-abstraction transfer reaction, which broadens the chain length distribution, but this does not occur for 1,2-butylene oxide (BO) under the conditions normally employed in the laboratory. In block copolymerizations, the chain length distribution may be widened as a result of slow initiation of the second block. This is a problem when ethylene oxide (EO) is added to an active B block, but not if the EO is polymerized first and the B block is formed subsequently.

In principle, a cationic-tipped copolymer could be prepared from a hydroxy-ended copolymer (*e.g.*, by bromination followed by reaction with an amine), but in practice it is difficult to achieve complete reaction without undesirable side reactions and/or chain scission. Potentially, the cleanest route is through use of a suitable functional initiator. An amine could be used to initiate oxyalkylene polymerization, but Hofmann elimination limits the molar mass achievable, broadens the distribution and gives rise to unsaturation.[13,14] In the work described here, we used aminoalcohols ($Me_2N(CH_2)_nOH$, n = 2,3), partially converted to their potassium alkoxide salts, employing a dry aprotic medium, tetrahydrofuran (THF).[15,16] Sequential anionic polymerization of EO followed by BO gave dimethylamino-tipped copolymers, samples of which were subsequently quaternized. Two aminoalcohols were used as starting points, 2-dimethylaminoethanol (DAE) and 3-dimethylaminopropan-1-ol (DAP).

Experimental

Polymerization

EO and BO (Fluka) were dried over powdered CaH_2. THF was dried by distillation from sodium–benzophenone under nitrogen. DAE (99.5%, Aldrich) was obtained already redistilled. DAP (Aldrich) was stored over molecular sieve 4 Å. Standard vacuum line techniques were used for the transfer of volatile monomers. Three preparation methods were employed in the course of this work.

Method 1, $Me_2N(CH_2)_2OE_{49}B_9$. DAE (0.38 g, 4.26 mmol) was added by syringe to freshly distilled THF (30 cm^3) in an ampoule under N_2. Potassium metal (*ca.* 0.09 g, 54 mol% DAE) was added piecewise to the stirred mixture over 1 h. The mixture was subjected to two freeze–pump–thaw cycles, then stirred overnight at ambient temperature to allow all of the potassium to react, giving a clear solution. EO (11.37 g, 60.55 mol equivalent DAE) was transferred into the ampoule under vacuum. After 5 days at a temperature of <27 °C, a thick white precipitate was observed. The temperature was gradually increased to 45 °C over a further 3 days, then a sample removed for analysis. THF was transferred out of the ampoule and BO (3.64 g, 12.60 mol equivalent DEA, allowing for sample removed) transferred in, under vacuum. The temperature was increased from 45 to 65 °C over 3 days. To neutralise the polymer it was dissolved in CH_2Cl_2 (750 cm^3 in total) and shaken with water. The mixture tended to form a thick white emulsion. The polymer was recovered by rotary evaporation and dried under vacuum (yield 13.27 g).

Method 2, $Me_2N(CH_2)_2OE_{58}B_7$ and $Me_2N(CH_2)_2OE_{39}B_{18}$. These polymers were prepared on a larger scale, but using a reduced proportion of potassium, for safety. Neutralisation of the copolymer was not attempted at this stage. The preparation of $Me_2N(CH_2)_2OE_{39}B_{18}$ is described. DAE (0.56 g, 6.28 mmol) was added by syringe to freshly distilled THF (25 cm^3) in an ampoule under N_2. Potassium metal (*ca.* 0.09 g, 37 mol% DAE) was added piecewise to the stirred mixture over 10 min. The mixture was subjected to two freeze–pump–thaw cycles, then stirred overnight at ambient temperature to allow all of the potassium to react, giving a clear solution. EO (16.73 g, 61.5 mol equivalent DAE) was transferred into the ampoule under vacuum. The temperature was gradually increased from ambient to 40 °C over 13 days, after which time a thick, white precipitate was observed. A sample was removed for analysis. THF was transferred out of the ampoule and BO (13.55 g, 32.3 mol equivalent DAE) transferred in, under vacuum. The temperature was increased from 48 to 58 °C over 7 days (yield 28.90 g).

Method 3, $Me_2N(CH_2)_2OE_{48}B_{22}$, $Me_2N(CH_2)_3OE_{79}B_{34}$ and $Me_2N(CH_2)_3OE_{26}B_{25}$. The first of these was prepared using DAE and the other two using DAP. The reason for moving to DAP was the thought that it might give polymers of higher stability. With DAE there was some concern that the quaternized polymer, with an alkoxy substituent β to the ammonium group, would be liable to β-elimination, although in practice this was not observed. In method 3 a nearly stoichiometric amount of potassium was used to try to eliminate the formation of olefinic by-products that were found with the method 2 copolymers. The scale of the reaction was reduced accordingly, for safety reasons. Potassium naphthalenide was used instead of potassium metal to generate the alkoxide, thus allowing more controlled formation of the alkoxide. THF, after distillation from sodium–benzophenone, was dried again over CaH_2, and THF was not removed prior to polymerization of the second monomer, BO. The preparation of $Me_2N(CH_2)_3OE_{26}B_{25}$ is typical. THF (30 cm^3) was transferred into an ampoule under vacuum and DAP (0.33 g) added by syringe. Potassium naphthalenide, prepared by dissolving potassium in THF containing a slight excess of naphthalene, was added until the green colour remained for a few seconds. The alkoxide was not completely soluble, a white precipitate was observed that did not disappear on stirring overnight at ambient temperature. EO (4.78 g, 34.4 mol equivalent DAP) was transferred into the ampoule under vacuum and the mixture stirred overnight. The ampoule was placed in a water bath and the temperature gradually increased from ambient to 47 °C over 10 days. A sample of the viscous, yellow solution was removed for analysis. BO (7.21 g, 31.2 mol equivalent DAP) was transferred into the ampoule under vacuum, then the temperature increased from 28 to 52 °C over 16 days. The naphthalene by-product was removed from the polymer by solvent extraction of a solution of the polymer in methanol (150 cm^3) with hexane (3 × 50 cm^3), toluene (4 × 50 cm^3) and hexane again (2 × 50 cm^3). The washings were back-extracted once to recover polymer lost during the washing process (yield 8.89 g).

Quaternization

The methylation of $Me_2N(CH_2)_2OE_{48}B_{22}$ is typical. $Me_2N(CH_2)_2OE_{48}B_{22}$ (4.58 g, 1.21 mmol) was dissolved in methanol (50 cm^3) in a conical flask. 2 M HCl (0.29 cm^3, 0.58 mmol) was added to neutralise the polymer. Methyl iodide (0.33 g, 2.33 mmol) was added and the mixture stirred overnight at ambient temperature, wrapped in foil. The mixture was washed with hexane (4 × 50 cm^3) and rotary-evaporated to dryness (yield 4.34 g, 91%). The reaction was monitored by thin-layer chromatography (TLC), using silica gel coated plates with an eluent of acetone : propan-2-ol : water (40 : 40 : 20 by volume). The plates were developed using iodine.

Copolymer characterization

Gel permeation chromatography (GPC) of dimethylamino-tipped copolymers was carried out in THF solvent at ambient temperature (Columns: Waters HR 1, 2 and 3). ^{13}C NMR

spectra of dimethylamino- and trimethylammonium-tipped copolymers were obtained in $CDCl_3$ using a Varian Unity 500 spectrometer.[17]

Silica synthesis

Silica was prepared following the procedure of Zhao *et al.*[18] Copolymer (0.20 g), distilled water (2.0 g) and 2 M HCl (8.0 g) were weighed into a 15 cm^3 sample tube. Tetraethoxysilane (TEOS) (1.04 g) was added to the polymer solution at the reaction temperature (60 °C or ambient temperature) and the tube shaken to mix the contents. The mixture was maintained overnight at the reaction temperature. The mother liquor was removed and the precipitate washed with water, until the washings were pH > 5. In some cases the water washings needed to be separated from the silica using a centrifuge. The precipitate was oven dried at 50 °C for 2 days. A portion was calcined for 2 h at 220 °C, then the temperature was increased at a rate of 1 °C min^{-1} to 400 °C, and maintained at that temperature for 6 h, under flowing air.

Silica characterization

X-Ray diffraction patterns were obtained using a Bruker D8 X-ray diffractometer in Bragg-Brentano geometry and CuKα1 radiation (λ = 0.154 nm).

Nitrogen adsorption–desorption isotherms were obtained using a Coulter SA3100 surface area analyser. Samples were outgassed for 16 h at 150 °C before analysis. BET surface area was calculated using data in the relative pressure range, p/p° = 0.05–0.2. Pore volume was calculated from the volume adsorbed at p/p° = 0.95. Mesopore radius, r_p, was calculated from the relative pressure (p/p°) corresponding to the step in the isotherm (attributed to capillary condensation), using

$$r_p = r_k + t. \quad (1)$$

Here, r_k is the core radius given by the Kelvin equation

$$r_k = -\frac{2\gamma V_L}{RT\ln(p/p^o)} \quad (2)$$

where γ is the surface tension and V_L the molar volume of the adsorbate, R is the universal gas constant and T is the absolute temperature. Statistical film thickness, t, was evaluated using an expression obtained by Kruk *et al.* from nitrogen adsorption measurements on MCM-41 samples[19]

$$t/\mathrm{nm} = 0.1\left[\frac{60.65}{0.03071 - \log_{10}(p/p^o)}\right]^{0.3968} \quad (3)$$

For suitable isotherms, micropore volumes were evaluated from t-plots.[20]

Results

Copolymer characterization

Average compositions from NMR end-group analysis and ratios of weight- to number-average molar mass, $\bar{M}_w/\bar{M}_n$, from GPC are given for the dimethylamino-tipped copolymers in Table 1. Assignments of ^{13}C NMR peaks associated with the terminal units of dimethylamino- and trimethylammonium-tipped copolymers are given in Table 2. Narrow molar mass distributions were achieved, but some samples contained by-products, as indicated in Table 1. Triblock copolymer (BEB) arises from traces of water present during the first stage and homopolymer (polyB) from traces of water during the second stage. An olefinic impurity was also present in some samples, which may arise from reaction of EO with the amine end of the aminoalcohol, giving a quaternary ammonium compound that could undergo β-elimination in the presence of base. The likelihood of this occurring is reduced if a high percentage of alcohol is converted to alkoxide, as in method 3 which gave polymers free of olefinic by-product, although with a slightly broader molar mass distribution. The polymers prepared by method 2, $Me_2N(CH_2)_2OE_{58}B_7$ and $Me_2N(CH_2)_2OE_{39}B_{18}$, were significantly contaminated with olefinic and other by-products. Attempts to purify these polymers by solvent extraction, reprecipitation and column chromatography were unsuccessful, so the mixtures arising from the polymerization were used subsequently in silica synthesis.

^{13}C NMR spectra of the quaternized polymers showed no sign of the starting material or of products that would result from methylation at the –OH end, suggesting that the methylation proceeded cleanly. Peaks due to olefinic impurities often disappeared during methylation, presumably due to reaction of the olefinic moiety with traces of iodine in the methyl iodide.

Silica characterization

Results from X-ray analysis of uncalcined and calcined silica products are presented in Table 3 and a representative X-ray

Table 1 Composition from ^{13}C NMR and polydispersity from GPC for dimethylamino-tipped oxyethylene–oxybutylene diblock copolymers

Code	Prep. method	Formula	$\bar{M}_w/\bar{M}_n$	By-products
CT63	1	$Me_2N(CH_2)_2OE_{49}B_9$	1.09	<10% olefinic
CT67	2	$Me_2N(CH_2)_2OE_{58}B_7$	1.07	9% BEB, 14% polyB, 20% olefinic
CT68	2	$Me_2N(CH_2)_2OE_{39}B_{18}$	1.06	5% BEB, 13% polyB, 22% olefinic
SA02	3	$Me_2N(CH_2)_2OE_{48}B_{22}$	1.14	
SA03	3	$Me_2N(CH_2)_3OE_{79}B_{34}$	1.10	
SA04	3	$Me_2N(CH_2)_3OE_{26}B_{25}$	1.13	

Table 2 ^{13}C NMR assignments for dimethylamino- and trimethylammonium-tipped oxyethylene–oxybutylene copolymers and olefinic by-products

Dimethylamino-tipped		Trimethylammonium-tipped		Olefinic by-product	
δ ($CDCl_3$, ppm)	Assignment	δ ($CDCl_3$, ppm)	Assignment	δ ($CDCl_3$, ppm)	Assignment
69.0	$-OCH_2CH_2NMe_2$	65.5 and 65.0	$-OCH_2CH_2NMe_3^+$	69.4 and 67.0	$-CH_2CH_2OCH{=}CH_2$
58.4	$-OCH_2CH_2NMe_2$			151.8	$-OCH{=}CH_2$
45.8	$-OCH_2CH_2NMe_2$	54.6	$-OCH_2CH_2NMe_3^+$	86.4	$-OCH{=}CH_2$
69.4	$-OCH_2CH_2CH_2NMe_2$	66.8	$-OCH_2CH_2CH_2NMe_3^+$		
27.7	$-OCH_2CH_2CH_2NMe_2$	24.0	$-OCH_2CH_2CH_2NMe_3^+$		
56.3	$-OCH_2CH_2CH_2NMe_2$	64.8	$-OCH_2CH_2CH_2NMe_3^+$		
45.3	$-OCH_2CH_2CH_2NMe_2$	53.6	$-OCH_2CH_2CH_2NMe_3^+$		

Table 3 X-Ray diffraction analysis of uncalcined and calcined silica products and weight loss on calcination

		Uncalcined silica					Calcined silica					
				Unit cell					Unit cell			
Structure-directing agent	Prep. temp./°C	*d*-spacing/nm	Probable structure	*a*/nm	*c*/*a*	*r*/nm	*d*-spacing/nm	Probable structure	*a*/nm	*c*/*a*	*r*/nm	Weight loss (%)
$Me_2HN^+(CH_2)_2OE_{49}B_9$	60	8.7	bcc	12.3	—	5.3	8.7	bcc	12.3	—	5.3	16
	Ambient	8.1, 5.7, 4.6	bcc	11.5	—	5.0	7.7, 5.5	bcc	10.9	—	4.7	23
$Me_2HN^+(CH_2)_2OE_{58}B_7$	60	8.5	bcc	12.0	—	5.2	8.4	bcc	11.9	—	5.1	29
	Ambient	8.3, 5.8, 4.7	bcc	11.7	—	5.1	8.4, 5.7	bcc	11.8	—	5.1	36
$Me_2HN^+(CH_2)_2OE_{39}B_{18}$	60	11.6, 7.2, 6.5, 6.4	3D-hex	14.7	2.0	7.4	11.7, 7.6, 6.3	3D-hex	14.5	2.1	7.3	30
	Ambient	14.6, 12.3, 6.7	3D-hex	15.9	1.9	8.0	11.9, 7.5, 6.7, 6.3	3D-hex	15.0	2.0	7.5	37
$Me_2HN^+(CH_2)_2OE_{48}B_{22}$	60	15.7, 9.1, 7.7, 5.9	3D-hex	18.1	2.2	8.7	13.4, 7.3, 5.6	3D-hex	16.8	2.0	8.4	38
$Me_2HN^+(CH_2)_3OE_{79}B_{34}$	60	17.9, 10.2, 5.8	3D-hex	23.4	1.7	11.7	17.9, 9.8, 7.6	3D-hex	22.7	1.8	11.4	40
$Me_2HN^+(CH_2)_3OE_{26}B_{25}$	60	12.7, 7.3, 6.5, 5.0	3D-hex	15.0	4.6	7.5	12.9, 7.5, 6.5	2D-hex	15.0	—	7.5	37
$Me_3N^+(CH_2)_2OE_{49}B_9$	60	9.1	bcc	12.9	—	5.6	9.0	bcc	12.7	—	5.5	21
	Ambient	15.2, 8.6, 6.8, 5.4	Cubic	15.2	—	7.6	7.9	bcc	11.2	—	4.8	34
$Me_3N^+(CH_2)_2OE_{58}B_7$	60	8.9	bcc	12.6	—	5.5	8.9	bcc	12.6	—	5.5	25
	Ambient	8.5	bcc	12.1	—	5.2	7.8	bcc	11.0	—	4.8	36
$Me_3N^+(CH_2)_2OE_{39}B_{18}$	60	15.5, 10.8, 6.5, 5.8	3D-hex	13.3	2.4	6.7	14.8, 10.8, 6.1, 5.7	3D-hex	13.3	2.3	6.7	34
$Me_3N^+(CH_2)_2OE_{48}B_{22}$	60	22.1, 14.4, 7.7	3D-hex	17.8	2.5	8.9	20.5, 14.6, 8.7	3D-hex	18.1	2.3	9.0	19
$Me_3N^+(CH_2)_3OE_{79}B_{34}$	60	18.1, 12.3, 9.9	3D-hex	22.8	2.0	11.4	17.9, 14.7, 9.8	3D-hex	22.6	2.0	11.3	29
$Me_3N^+(CH_2)_3OE_{26}B_{25}$	60	12.0, 8.9, 7.1, 6.1	3D-hex	14.0	2.9	7.0	11.8, 7.0, 6.7, 6.1	3D-hex	14.1	2.9	7.1	39

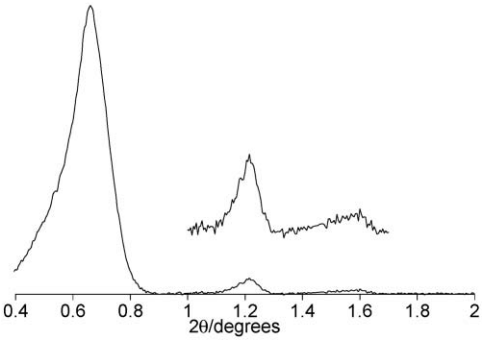

Fig. 1 X-Ray pattern for calcined silica prepared with $Me_2HN^+(CH_2)_2OE_{48}B_{22}$.

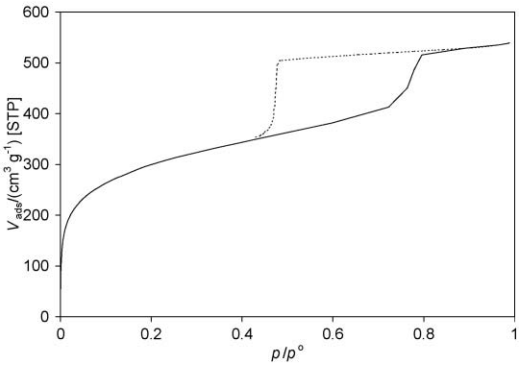

Fig. 2 Nitrogen adsorption (—) and desorption (– – –) isotherm for calcined silica prepared with $Me_2HN^+(CH_2)_2OE_{48}B_{22}$.

pattern is shown in Fig. 1. With structure-directing agents that have relatively small hydrophobic blocks (B_7 and B_9), silica prepared at 60 °C exhibited only a single X-ray peak. However, silica prepared at ambient temperature often gave more detailed X-ray patterns. Equivalent nonionic polymers are known to form bcc structures (space group *Im*3*m*) of packed spherical micelles in neutral aqueous solution,[12] and this structure has tentatively been assigned to silica generated with the B_7 and B_9 copolymers. Silica formed at ambient temperature with $Me_3N^+(CH_2)_2OE_{49}B_9$, as synthesised, appeared to have a particularly expanded cubic structure, which contracted significantly on calcination. With structure-directing agents that have longer hydrophobic blocks (B_{18}, B_{22}, B_{25} and B_{34}), silica was formed that gave X-ray patterns consistent with a hexagonal structure. In most cases, this appeared to be a three-dimensional hexagonal structure (3D-hex), which may be similar to that of SBA-12 (assigned space group $P6_3/mmc$).[18] The 3D-hex structure may arise from packing of elongated micelles. It has been found previously that the nonionic copolymer $E_{18}B_{10}$, which has a similar proportion of E, may form elongated micelles.[21] For $Me_2HN^+(CH_2)_3OE_{26}B_{25}$, silica prior to calcination exhibited a 3D-hex structure with an extended unit cell ($c/a = 4.6$), which on calcination developed into a two-dimensional hexagonal structure (2D-hex, space group *P*6*mm*). Values of radius ('pore' + ½ 'pore wall'), *r*, calculated on the basis of probable structures, are included in Table 3.

Weight losses on calcination are also given in Table 3. It can be seen that in general weight losses were greater for silica prepared at ambient temperature than for silica prepared at 60 °C. It is probable that during calcination, in addition to degradation of the structure-directing agent, there is further condensation of silica. The greater weight losses for silica prepared at ambient temperature indicate, as might be expected, a lower degree of condensation prior to calcination.

Calcined silica products exhibited Type IV nitrogen adsorption–desorption isotherms with type H2 hysteresis, indicative of mesoporous materials.[22] A representative isotherm is shown in Fig. 2 and results of nitrogen adsorption analysis are listed in Table 4. High values of BET surface area, *A*, and pore volume, V_{pore}, were generally achieved. It has been noted previously that silica formed under acid conditions in the presence of a block copolymer structure-directing agent exhibits a degree of microporosity.[11,23,24] For suitable isotherms, values of micropore volume, V_{micro}, were evaluated from *t*-plots. It can be seen in Table 4 that only a modest portion of the total pore volume is in the micropores, although this may represent a significant contribution to the surface area. For the silica prepared from $Me_3N^+(CH_2)_2OE_{48}B_{22}$, calcination may have been incomplete, as evidenced by low values of *A* and V_{micro} and low weight loss on calcination, so these results are excluded from the following discussion. Values of mesopore radius, r_{pore}, evaluated from the position of the step in the isotherm, $(p/p^\circ)_{step}$, are included in Table 4.

BET surface areas are plotted in Fig. 3, which also indicates how decreasing the mole fraction of hydrophilic units promotes transitions from cubic to three-dimensional hexagonal to two-dimensional hexagonal structures. It can be seen in Fig. 3 that surface areas generally increase in the sequence nonionic

Table 4 Nitrogen adsorption analysis of calcined silica products: BET surface area, A, total pore volume, V_{pore}, micropore volume, V_{micro}, position of step in isotherm, $(p/p^{\circ})_{step}$, and calculated mesopore radius, r_p

Structure-directing agent	Prep. temp./°C	A/m^2 g^{-1}	V_{pore}/cm^3 g^{-1}	V_{micro}/cm^3 g^{-1}	$(p/p^{\circ})_{step}$	r_p/nm
$Me_2HN^+(CH_2)_2OE_{49}B_9$	60	948	0.58		0.52	2.3
	Ambient	968	0.60		0.54	2.4
$Me_2HN^+(CH_2)_2OE_{58}B_7$	60	1033	0.64		0.52	2.3
	Ambient	879	0.43		0.40	1.8
$Me_2HN^+(CH_2)_2OE_{39}B_{18}$	60	977	0.84	0.16	0.76	4.5
	Ambient	982	0.82	0.20	0.76	4.5
$Me_2HN^+(CH_2)_2OE_{48}B_{22}$	60	1078	0.83	0.29	0.78	4.9
$Me_2HN^+(CH_2)_3OE_{79}B_{34}$	60	1118	0.90	0.34	0.83	6.3
$Me_2HN^+(CH_2)_3OE_{26}B_{25}$	60	878	0.97	0.16	0.78	4.9
$Me_3N^+(CH_2)_2OE_{49}B_9$	60	863	0.71		0.60	2.7
	Ambient	980	0.59		0.52	2.3
$Me_3N^+(CH_2)_2OE_{58}B_7$	60	879	0.52		0.53	2.3
	Ambient	773	0.40		0.40	1.8
$Me_3N^+(CH_2)_2OE_{39}B_{18}$	60	736	0.53	0.14	0.65	3.1
$Me_3N^+(CH_2)_2OE_{48}B_{22}$	60	480	0.56	0.01	0.79	5.2
$Me_3N^+(CH_2)_3OE_{79}B_{34}$	60	817	0.75	0.19	0.84	6.7
$Me_3N^+(CH_2)_3OE_{26}B_{25}$	60	851	0.87	0.22	0.76	4.5

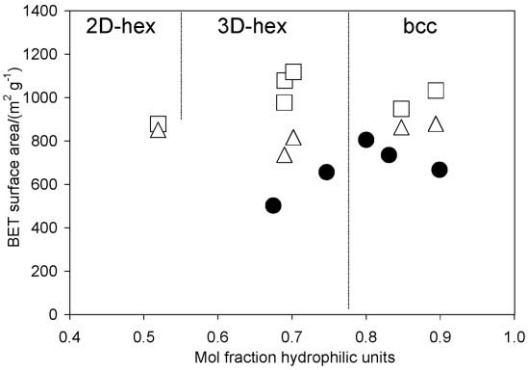

Fig. 3 BET surface area and probable structure for calcined silica prepared with nonionic (●), dimethylamino-tipped (□) and trimethylammonium-tipped (△) oxyethylene–oxybutylene diblock copolymers with various mol fraction hydrophilic units.

< trimethylammonium-tipped < dimethylamino-tipped. The very high surface areas obtained with dimethylamino-tipped structure-directing agents reflect relatively high micropore volumes (Table 4).

Discussion

We have previously studied the structure-directing effects of five nonionic E–B diblock copolymers ($E_{40}B_{10}$, $E_{54}B_{11}$, $E_{89}B_{10}$, $E_{56}B_{19}$ and $E_{56}B_{27}$).[11] $E_{40}B_{10}$ and $E_{54}B_{11}$ gave silica which could be assigned a bcc structure. Further work with $E_{56}B_{19}$ and $E_{56}B_{27}$ has given silica which can be assigned a 3D-hex structure. We have demonstrated for these nonionic copolymers that the dimensions of the silica mesostructure scale with the expected micelle dimensions.[11] Neutron scattering experiments on micelles formed from similar E_mB_n copolymers have indicated that in the micelle corona the dimensions of the E chain are approximately twice its radius of gyration, whilst in the core the B chain is stretched to about 60% of its fully extended length.[12,21] The ratio of corona size to core radius is thus expected to be of the order of $2.1m^{1/2}/n$. Since, for the hydrophobic block, the fully extended length per B unit is 0.36 nm, a micelle core radius, r_{core}, may be calculated as

$$r_{core}/\text{nm} = 0.216n \quad (4)$$

and an overall micelle radius, $r_{micelle}$, as

$$r_{micelle}/\text{nm} = r_{core} + 0.454m^{1/2}. \quad (5)$$

These equations are based on a limited number of empirical

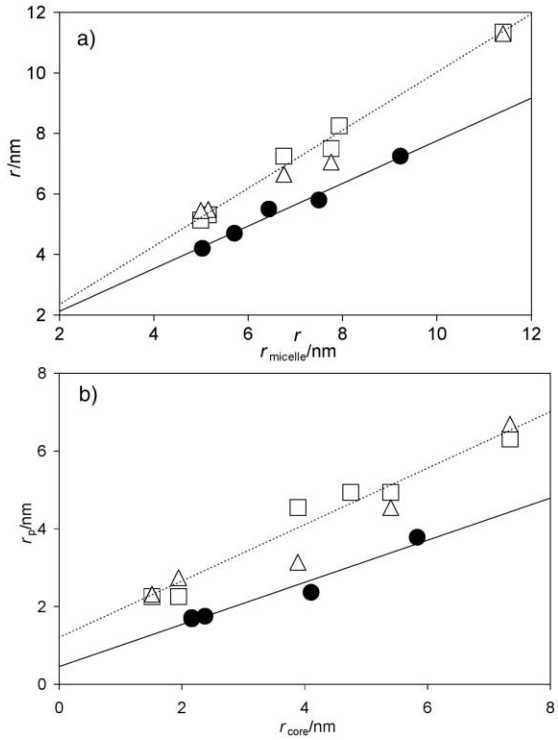

Fig. 4 Dependence of (a) effective radius ('pore' + ½ 'pore wall'), r, for the silica mesostructure, determined from X-ray scattering data for calcined silica products, on calculated micelle radius, $r_{micelle}$, and (b) mesopore radius, r_p, determined from nitrogen adsorption data for calcined silica products, on calculated micelle core radius, r_{core}, for nonionic (●), dimethylamino-tipped (□) and trimethylammonium-tipped (△) oxyethylene–oxybutylene diblock copolymers.

data, and will not necessarily apply over a very wide range of copolymer compositions. Nevertheless, they provide a basis for making initial predictions.

In Fig. 4(a) the effective radius ('pore' + ½ 'pore wall'), r, for the silica mesostructure, determined from X-ray scattering data for calcined silica products, is plotted against $r_{micelle}$. In Fig. 4(b) the mesopore radius, r_p, determined from nitrogen adsorption data for calcined silica products, is plotted against r_{core}. It can be seen in Fig. 4 that the dimensions of the silica mesostructure are related to the overall micelle size, and that the mesopore dimensions are related to the size of the hydrophobic micelle core. The suggests a simple model in which the hydrophilic chains are embedded in the silica walls in the uncalcined silica, generating micropores on calcination,

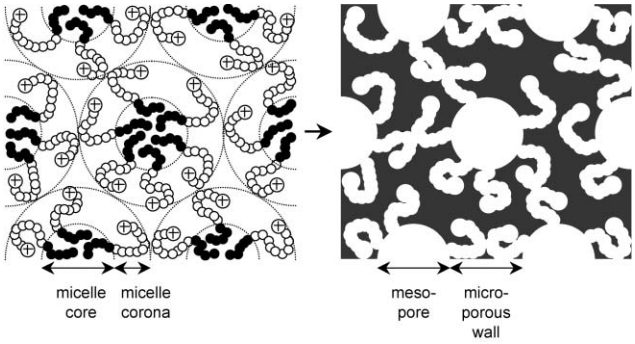

Fig. 5 Schematic illustration of a packed micelle structure, in which silica penetrates the corona region, giving on calcination a mesoporous material with microporous walls.

whilst the hydrophobic chains form a separate microphase, giving rise to mesopores on calcination (Fig. 5). Göltner, Smarsly and colleagues have drawn similar conclusions for mesoporous silica prepared by nanocasting with nonionic surfactants and have demonstrated that molecularly dissolved poly(oxyethylene) may give rise to microporosity.[23–25] It is feasible that a portion of the hydrophilic block also contributes to the mesopores.[23]

It can also be seen in Fig. 4 that the dimethylamino- and trimethylammonium-tipped copolymers, all of which carry a positive charge under the acidic conditions of the silica synthesis, give silica with larger mesostructure dimensions [Fig. 4(a)] and larger mesopore sizes [Fig. 4(b)] than equivalent nonionic copolymers. This suggests that the charged tip gives rise to additional expansion of the copolymer chains, which may be attributed to repulsion between charged groups and increased micelle hydration. Eqns. (4) and (5) should thus be modified for E–B copolymers with charged tips, and further work is required to elucidate the influence of a charged tip on the solution properties and micellization behaviour of E–B block copolymers.

Conclusions

This work has demonstrated that:

(1) Dimethylamino-tipped E–B diblock copolymers can be prepared through use of aminoalcohol initiators. The formation of unwanted by-products is reduced if a high percentage of the alcohol is converted to alkoxide. Trimethylammonium-tipped E–B diblock copolymers may be generated by subsequent quaternization.

(2) When E–B block copolymers are utilised as structure-directing agents in the preparation of mesoporous silica, the structure obtained is controlled primarily by the proportion of hydrophilic units in the copolymer, the dimensions of the silica mesostructure are controlled primarily by the overall micelle size and the mesopore dimensions are controlled primarily by the size of the hydrophobic micelle core.

(3) The addition of a charged tip to the hydrophilic block results in an expansion of the structure obtained and in higher surface areas for calcined silica products.

Acknowledgement

CET is grateful to the Daphne Jackson Trust for the award of a research fellowship, funded by EPSRC. SJA is grateful to EPSRC for provision of an advanced course (MSc) studentship. Thanks are due to Dr C. Booth, Dr F. Heatley and Dr C. Chaibundit (Chemistry, University of Manchester) and to Mr B. Smith (Earth Sciences, University of Manchester) for helpful discussions.

References

1 I. W. Hamley, *The Physics of Block Copolymers*, Oxford University Press, Oxford, 1998.
2 C. Booth and D. Attwood, *Macromol. Rapid Commun.*, 2000, **21**, 501.
3 H. Altinok, S. K. Nixon, P. A. Gorry, D. Attwood, C. Booth, A. Kelarakis and V. Havredaki, *Colloids Surf., B*, 1999, **16**, 73.
4 Y. A. I. Abu-Lebdeh, P. M. Budd and V. M. Nace, *J. Mater. Chem.*, 1998, **8**, 1839.
5 H. B. S. Chan, P. M. Budd and T. d. V. Naylor, *J. Mater. Chem.*, 2001, **11**, 951.
6 C. T. Kresge, M. E. Leonowicz, W. J. Roth, J. C. Vartuli and J. S. Beck, *Nature*, 1992, **359**, 710.
7 J. S. Beck, J. C. Vartuli, W. J. Roth, M. E. Leonowicz, C. T. Kresge, K. D. Schmitt, C. T. W. Chu, D. H. Olson and E. W. Sheppard, *J. Am. Chem. Soc.*, 1992, **114**, 10834.
8 S. A. Bagshaw, E. Prouzet and T. J. Pinnavaia, *Science*, 1995, **269**, 1242.
9 D. Y. Zhao, P. D. Yang, N. Melosh, Y. L. Feng, B. F. Chmelka and G. Stucky, *Adv. Mater.*, 1998, **10**, 1380.
10 D. Zhao, J. Feng, Q. Huo, N. Melosh, G. H. Frederickson, B. F. Chmelka and G. D. Stucky, *Science*, 1998, **279**, 548.
11 C. E. Tattershall, N. P. Jerome and P. M. Budd, *J. Mater. Chem.*, 2001, **11**, 2979.
12 I. W. Hamley, C. Daniel, W. Mingvanish, S.-M. Mai, C. Booth, L. Messe and A. J. Ryan, *Langmuir*, 2000, **16**, 2508.
13 K. S. Kazanskii and N. V. Ptitsyna, *Vysokomol. Soedin., Ser. B*, 1987, **29**, 351.
14 K. S. Kazanskii and N. V. Ptitsyna, *Makromol. Chem.*, 1989, **190**, 255.
15 M. Mosquet, Y. Chevalier, P. Le Perche and J. P. Guicquero, *Macromol. Chem. Phys.*, 1997, **198**, 2457.
16 Y. Wang, S. Chen and J. Huang, *Macromolecules*, 1999, **32**, 2480.
17 F. Heatley, G.-E. Yu, W.-B. Sun, E. J. Pywell, R. H. Mobbs and C. Booth, *Eur. Polym. J.*, 1990, **26**, 583.
18 D. Zhao, Q. Huo, J. Feng, B. F. Chmelka and G. D. Stucky, *J. Am. Chem. Soc.*, 1998, **120**, 6024.
19 M. Kruk, M. Jaroniec and A. Sayari, *Langmuir*, 1997, **13**, 6267.
20 S. J. Gregg and K. S. W. Sing, *Adsorption, Surface Area and Porosity*, Academic Press, London, 1982.
21 L. Derici, S. Ledger, S.-M. Mai, C. Booth, I. W. Hamley and J. S. Pedersen, *Phys. Chem. Chem. Phys.*, 1999, **1**, 2773.
22 K. S. W. Sing, D. H. Everett, R. A. W. Haul, L. Moscou, R. A. Pierotti, J. Rouquerol and T. Siemieniewska, *Pure Appl. Chem.*, 1985, **57**, 603.
23 C. G. Göltner, B. Smarsly, B. Berton and M. Antonietti, *Chem. Mater.*, 2001, **13**, 1617.
24 B. Smarsly, C. Göltner, M. Antonietti, W. Ruland and E. Hoinkis, *J. Phys. Chem. B*, 2001, **105**, 831.
25 B. Smarsly, S. Polarz and M. Antonietti, *J. Phys. Chem. B*, 2001, **105**, 10473.